Journal of Metals, Materials and Minerals, 35(2), e2185, 2025

Tin oxide nanoparticle extraction from waste solder dross via low-temperature hydrometallurgical process

Tanongsak YINGNAKORN[1], Sirunya SOMLA[1], Thanapon CHANDAKHIAW[1], Ethan CHEUNG[2], and Sakhob KHUMKOA[1,*]

[1] *School of Metallurgical Engineering, Suranaree University of Technology, Nakhon Ratchasima 30000, Thailand*
[2] *School of Chemistry, University of Leicester, Leicester, LE1 7RH, United Kingdom*

***Corresponding author e-mail**: sakhob@sut.ac.th

Received date:
19 October 2024
Revised date:
27 March 2025
Accepted date:
14 May 2025

Keywords:
SnO_2;
Nanoparticles;
Tin oxide nanoparticles;
Solder dross;
Hydrometallurgy

Abstract

This study proposes a hydrometallurgical approach to valorising industrial waste by producing SnO_2 nanoparticles (NPs) from waste solder dross obtained by skimming off of tin solder baths from electronic dipping processes. The process involves leaching the dross with aqueous hydrochloric acid solution and hydrogen peroxide, followed by precipitation with ammonium hydroxide and purification with aqueous nitric acid solution. The optimised leaching conditions were determined to be 4 mol· L^{-1} HCl, 11% v/v H_2O_2, 25°C, and a leaching time of 15 min. SnO_2 NPs were successfully precipitated at pH 4 using 25% v/v NH_4OH and purified with 1 mol· L^{-1} HNO_3. The whole process was able to recover nearly 100% of tin from waste solder dross as SnO_2 NPs, with a high purity of 99.5% and a particle size distribution of ca. 2 nm to 7 nm. The overall material balance and the simple cost of the process were evaluated to provide an idea of the economic viability and the possibility of scaling up the method detailed in this work.

1. Introduction

Tin-based solder alloys, renowned for their desirable properties, such as excellent electrical conductivity, high corrosion resistance, mechanical strength, affordability, and low melting point, have widespread application in bonding workpieces and metals, particularly in the electronics industry [1,2]. These alloys are broadly categorised into two main groups: lead-containing (Sn-Pb) solder and lead-free solder. However, the environmental and health concerns associated with lead exposure led to the prohibition of traditional lead-based solder by the European Union (EU) in July 2006. Subsequently, the Restriction of Hazardous Substances (RoHS) directive mandated the phase-out of lead in electronic products [3]. This regulatory framework has also been used in numerous countries, including China, Japan, South Korea, and the United States, to mitigate the risks caused by lead-containing solder [1,4]. As a result, the development of lead-free solder alternatives became imperative. Typical compositions of lead-free tin-based solders include Sn–Bi–Ag, Sn–Bi, Sn–Zn, Sn–Ag–Cu, Sn–Cu, and Sn–Zn–Bi, which often exhibit properties comparable to their lead-containing solder [4-6].

These lead-free tin-based solders are primarily used in dip soldering; a simple process in which electronic components are submerged in a molten solder bath for joining. The large surface area of the molten solder bath is exposed to air at high temperatures of 260°C to 270°C, forming a solder oxide layer on the surface [7]. This oxide layer, known as 'dross', is periodically skimmed off to keep the solder clean of any impurities [7,8]. Dross typically contains 60 wt% to 90 wt% of valuable metals such as tin, copper, and silver in their oxide forms, depending on the composition of the solder alloy [7].

Many studies have focused on the recovery of these valuable metals from dross through various metallurgical techniques, including pyrometallurgy, hydrometallurgy, and electrometallurgy. One commonly employed method for recovering solder metals from dross is carbothermic reduction. In this process, the dross is mixed with a carbon source, such as coke, graphite, or calcium carbonate, and heated to temperatures exceeding 600°C [8,9]. This reaction reduces the metal oxides to their metallic form, resulting in a molten metal phase. However, this process often generates a second dross that requires further treatment. Both the original dross collected from the solder bath and the secondary dross produced during the recovery process can be further treated using hydrometallurgical and electrometallurgical methods to extract valuable metals. For instance, the waste solder can be leached using nitric acid (HNO_3) or hydrochloric acid (HCl) [8,10-12]. The resulting solution can then be treated to separate silver or silver compounds through selective leaching, precipitation, or cementation techniques. Subsequently, copper and tin can be recovered from the solution using electrowinning processes [11,12].

Tin exhibits two common oxidation states, divalent (Sn^{2+}) and tetravalent (Sn^{4+}). This dual valency leads to forming two primary oxides: stannous oxide (SnO) and stannic oxide (SnO_2). While both oxides are possible, SnO_2 is thermodynamically more stable [13,14] and can be used in many different applications, such as antimicrobial, anti-oxidant, lithium batteries, solar panels, supercapacitors, catalysis, gas sensors, and cleaning agents. SnO_2 can also be produced into nano-

DOI:10.55713/jmmm.v35i2.2185

particles (NPs) through various synthetic routes that are utilised in literature and industry. These SnO_2 NPs share many similar applications to their bulk form, such as use in electronics, solar panels, and catalysis [13,15,16]. For example, SnO_2 NPs can be synthesised via precipitation methods using precursors like $SnCl_4 \cdot 5H_2O$ or $SnCl_4 \cdot 2H_2O$ and precipitating agents such as NH_4OH or NaOH [14,17]. These approaches allow for the production of nanoparticles with sizes ranging from 2 nm to 25 nm [18-21]. Therefore, this study proposes a novel approach and aims to synthesise valuable SnO_2 NPs from industrial lead-free solder dross, a waste product of electronic dipping processes. The proposed method involves leaching tin from the solder dross followed by SnO_2 NP precipitation using various precipitating agents, including NH_4OH and NaOH. While the raw material contains impurities such as copper and zinc, these metals will be removed during the processing steps.

2. Experimental

2.1 Materials

The waste solder dross obtained from dip soldering baths for the electric wire dipping process was provided by a company in Thailand. The chemicals used in this study were hydrochloric acid (commercial HCl, ITALMAR, 35%), hydrogen peroxide (H_2O_2, QReC, 35%), ammonium hydroxide (NH_4OH, ITALMAR, 25% commercial grade), and sodium hydroxide (NaOH, RCL Labscan, 99%).

2.2 Synthesis of SnO_2 nanoparticles

As depicted in Figure 1, the raw lead-free solder dross material (1 kg) was subjected to a leaching process using aqueous solutions of hydrochloric acid at a 0.1 solid to liquid (S/L) ratio of the tin solder dross to aqueous solutions of hydrochloric acid with varying concentrations (0.5 $mol \cdot L^{-1}$ to 4 $mol \cdot L^{-1}$), hydrogen peroxide volume ratios (5% to 12% v/v), temperatures (25°C to 90°C), and leaching durations (5 min to 120 min). All experimental conditions were stirred with a head stirrer. The optimal conditions were then employed for the precipitation of SnO_2 NPs. Ammonium hydroxide (25%) and sodium hydroxide (1 $mol \cdot L^{-1}$) were compared as precipitating agents with different pH values. The precipitated nanoparticles were separated via centrifugation (5 min at 8,000 rpm), followed by washing with reverse osmosis (RO) water (0.1 S/L ratio) and drying (24 h at 60°C). To ensure the purity of the nanoparticles, a meticulous process of removing copper contamination was undertaken. This involved leaching the nanoparticles with nitric acid aqueous solution (1 $mol \cdot L^{-1}$, 0.1 S/L ratio), followed by centrifugation (5 min at 8,000 rpm) and washing with RO water (0.1 S/L ratio). A final centrifugation step (5 min at 8,000 rpm) was performed prior to drying (24 h at 60°C).

2.3 Instrumentation (Characterisation)

Wavelength-dispersive X-ray fluorescence (WD-XRF) analysis was performed using a Panalytical AXIOS MAX instrument. Solid tin solder dross samples were ground into fine particles and analysed under the control of SuperQ software. X-ray diffraction (XRD) patterns were acquired using a Bruker D2 PHASER X-ray generator operating at 30 kV and 10 mA. DIFFRAC.SUITE software was employed for instrument control. Samples were prepared in polymethyl methacrylate (PMMA) specimen holders and scanned over a 2θ range of 10° to 90° with a step size of 0.02°. Scanning electron microscopy (SEM) and energy dispersive X-ray spectroscopy (EDS) analysis of the samples was conducted using a JEOL JSM-6010LV instrument operating at 10 kV to 15 kV and a spot size of 35 nm. The morphology and elemental mapping were assessed using InTouchScope™ software for image acquisition and INCAEnergy EDS software for chemical analysis. The NP size was analysed by a Talos F200X G2 (Thermo Scientific) transmission electron microscopy (TEM) with an accelerating voltage of 200 kV. The initial sample was added in 1 mL of ethanol and distributed as a colloidal suspension in an ultrasonic bath, followed by dropping onto a copper grid, which was dried in a desiccator cabinet overnight before analysing with TEM. Inductively coupled plasma-optical emission spectrometry (ICP-OES) was utilised for the elemental analysis of solutions. Prior to analysis, samples were diluted with 2% nitric acid to ensure analyte concentrations were within the calibration range of 0.05 ppm to 10 ppm.

3. Results and discussion

The waste solder dross generated in this study, as depicted in Figure 2(a), primarily consists of Sn (86.52 wt%), O (9.54 wt%), Cu (2.56 wt%) and Zn (0.79 wt%), with trace amounts of Cl detected through the SEM-EDS analysis presented in Figure 2(b). The presence of Cu in the waste solder dross is likely attributed to contamination from the dipping process of copper electric wires. This raw solder dross material served as the feedstock for the hydrometallurgical process developed in this study, aimed at recovering tin and synthesising SnO_2 NPs.

Hydrochloric acid (HCl) is an extensive reagent in various industrial sectors, such as metallurgy, woodworking, textile dyeing, and petroleum processing [22,23]. Given its potential to leach metals such as tin and copper, we employed an aqueous HCl solution as a suitable medium for the waste solder dross leaching [12,24]. Concurrently, hydrogen peroxide, a potent oxidant with minimal toxicity at low concentrations, was employed as a reactive additive to enhance the leaching process [25]. To optimise the leaching efficiency of solder dross in HCl aqueous solutions, the influence of various parameters was investigated (Figure 3).

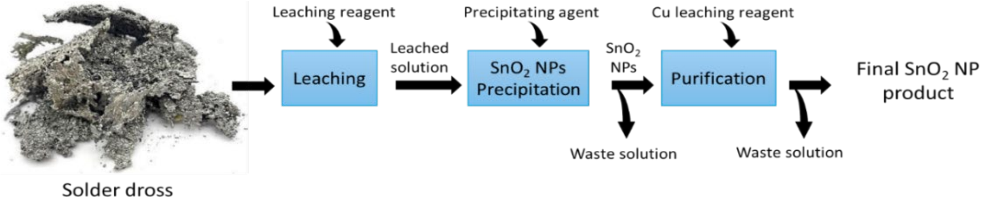

Figure 1. Schematic diagram showing the experimental procedure applied in this study to produce tin oxide nanoparticles from waste lead-free solder dross.

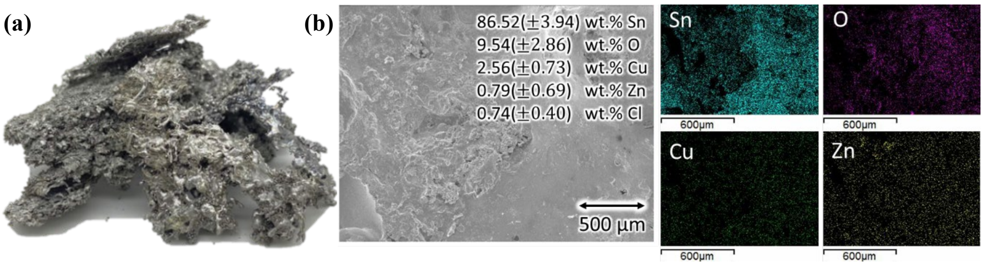

Figure 2. (a) Image of the raw tin solder dross material and (b) SEM-EDS images of raw tin solder dross material used in this study (see Figure S1 for full mapping version).

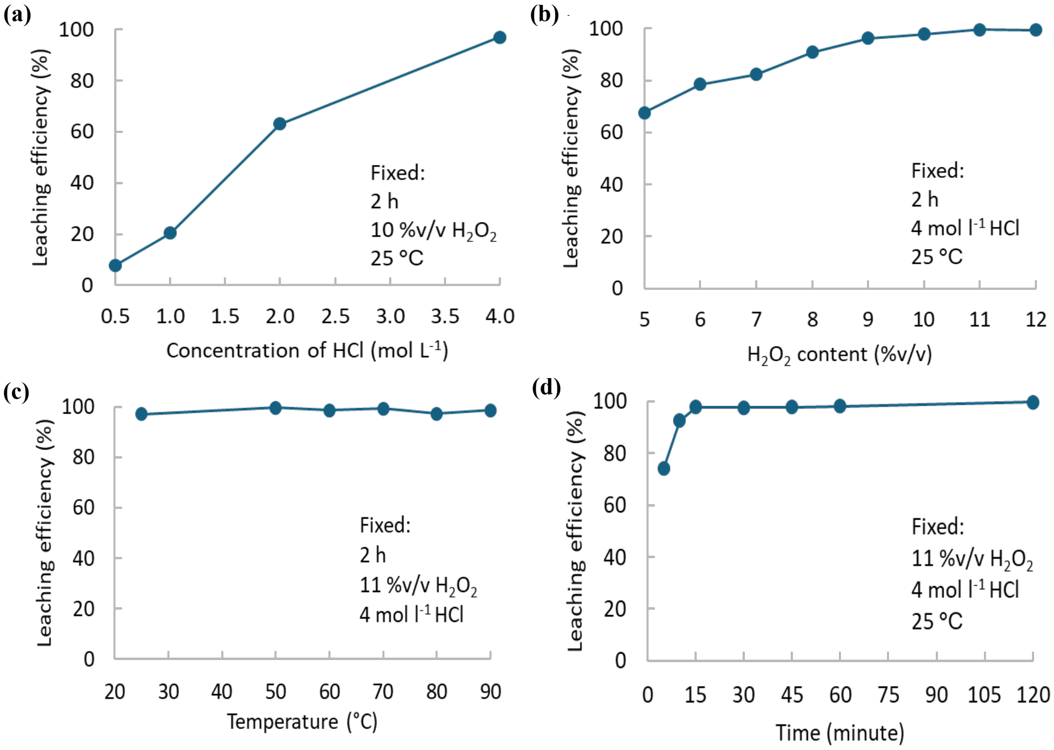

Figure 3. Effect of increasing (a) HCl concentration, (b) H_2O_2 volume, (c) temperature, and (d) time on waste solder dross leaching in HCl aqueous solutions at a 0.1 S/L ratio of tin solder dross to HCl aqueous solution.

Leaching efficiency was determined by comparing the residual mass after leaching to the initial mass of the solder dross for all conditions. The effect of HCl concentration on leaching efficiency was evaluated at a fixed 0.1 S/L ratio of tin solder dross to HCl aqueous solution, with an addition of 10% v/v H_2O_2 reducing agent, a temperature of 25°C, and a leaching time of 2 h (Figure 3(a)). A strong positive correlation between HCl concentration and leaching efficiency is observed, leading to the selection of a 4 mol·L^{-1} HCl concentration for further experiments. Subsequently, the impact of H_2O_2 concentration was examined (Figure 3(b)). While increasing H_2O_2 concentration initially improves leaching efficiency, a plateau is reached at 11% v/v, indicating near-complete leaching. Therefore, 11% v/v H_2O_2 is chosen for subsequent experiments. The effect of temperature on leaching efficiency was then evaluated (Figure 3(c)). Despite an initial increase in efficiency with higher temperatures, no significant changes are observed beyond 25°C, likely due to the already high leaching efficiency and thus, the temperature remains unchanged at 25°C for the following experiments. Finally, the influence of leaching time was investigated (Figure 3(d)). Results indicated that a leaching time of 15 min is sufficient to achieve optimal efficiency. Based on these findings, the optimised leaching conditions for solder dross were determined to be 4 mol·L^{-1} HCl, 11% v/v H_2O_2, 25°C, and a leaching time of 15 min at a 0.1 S/L ratio of solder dross sample to HCl aqueous solution.

To precipitate SnO_2 NPs from the leached solution, NH_4OH (25%) and NaOH (1 mol·L^{-1}) aqueous solutions were employed as precipitating agents. The leached solution contains ca. Sn (86,000 mg·L^{-1}), Cu (1,200 mg·L^{-1}), and trace amounts (lower than 100 mg·L^{-1}) of other metals such as Zn, Fe, and Al at a pH of nearly 0. The effects of pH on metal ion concentrations in solution and the characteristics of the precipitated powder were evaluated (Figure 4). The NH_4OH and NaOH (1 mol·L^{-1}) aqueous solutions were added to adjust the pH, and the resulting solutions were analysed using ICP-OES. The precipitated powders were characterised by XRD after centrifugation, rinsing with RO water, and drying. As demonstrated in Figure 4(a), the tin metal ion is shown to have near 100% precipitation from the leached solution by adjusting the pH to 4 using a 25% v/v NH_4OH solution. The resulting precipitate was characterised as SnO_2 by XRD analysis (Figure 4(c)). While this method effectively selectively precipitated tin from the solution, it also precipitated a small portion of the copper ions (zinc is not significantly precipitated at pH 4 in this step, as shown in Figure S2). Consequently, a subsequent purification step was necessary to isolate pure tin nanoparticles. Additionally, precipitation at higher pH values is deemed unnecessary due to the presence of SnO peaks (see Figure S3 for more details) in the XRD patterns (Figure 4(c)) and dark-grey colour caused by the increased presence of SnO [26], which are undesirable for tin oxide nanoparticle applications due to lower stability and electronic bandgap[13,14,27]. Moreover, increasing the pH requires a larger volume of the precipitation agent.

Alternatively, precipitation using NaOH solution (1 mol·L^{-1}) could also be employed to remove tin ions from the leached solution (Figure 4(b)). However, this method necessitated a significantly larger volume of NaOH solution to achieve complete precipitation of tin. For instance, ca. 285% v/v of NaOH solution was required to precipitate SnO_2 NPs at pH 3 (Figure 4(b) and Figure 4(d)) with nearly 100% efficiency, which is significantly higher than the volume of NH_4OH solution required for the same precipitating process. This increased consumption of NaOH is undesirable from a process efficiency standpoint due to the generation of secondary solution waste. Given these considerations, precipitation with NH_4OH solution at pH 4 was selected for further investigation.

Next, we successfully purified the SnO_2 NPs contaminated with copper using HNO_3 aqueous solutions. While tin oxides are insoluble in HNO_3 aqueous solutions, this reagent is known for its effectiveness in Cu leaching [11,28]. Consequently, this study employed a 1 mol·L^{-1} HNO_3 aqueous solution as a selective leaching agent for Cu removal. The process, visually indicated by a colour change from the original solution to a vibrant blue (a characteristic of Cu nitrate) [29], is completed within ca. 6 h. This step effectively removes the copper impurity, significantly enhancing the purity of the SnO_2 NPs for its potential applications. The nanoparticles are then separated from the solution through centrifugation (5 min, 8,000 rpm) and dried. The removal of copper resulted in a noticeable colour change from bright yellow to milky white, and no significant change occurred to the SnO_2 NP structure before and after Cu removal, as depicted in the XRD patterns shown in Figure 5(a). The morphological characteristics of the purified SnO_2 NPs are examined using SEM and TEM (Figure 5(b-c)), revealing a particle size distribution of 3.24 nm (see size distribution in Figure S4) with lattice fringes spacing ca. 3.3 Å, corresponding to the c axis dimension of rutile structured SnO_2 [30]. The WD-XRF analysis is conducted to determine the chemical composition of the SnO_2 NPs before and after the copper removal process (Table 1). The Sn:O atomic ratio is 1:2, which is relative to the SnO_2 structure

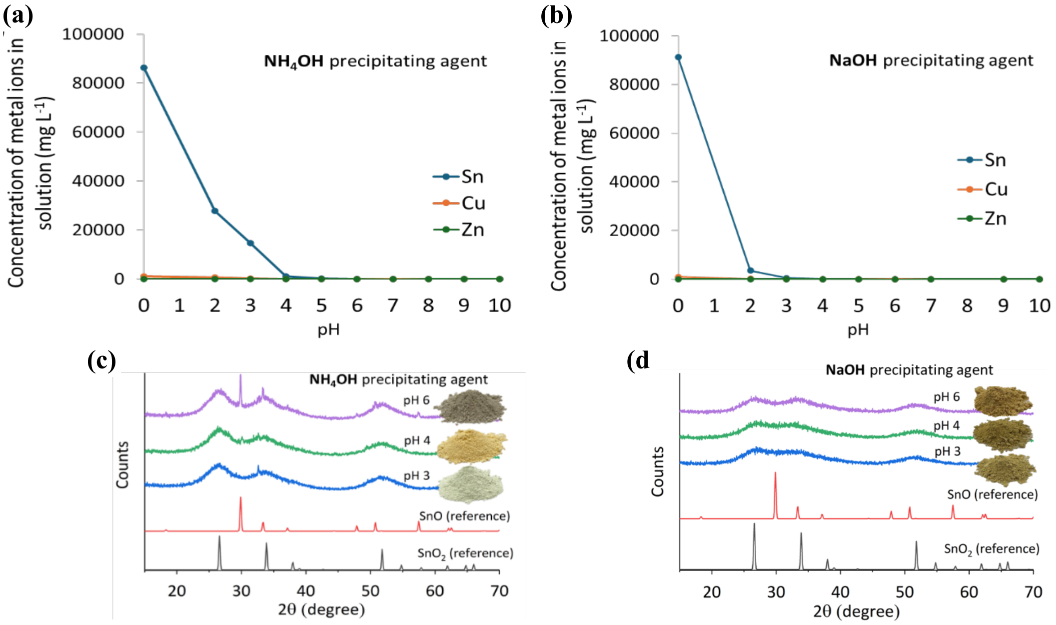

Figure 4. The concentration of SnO_2 NPs precipitated from the metal ion solution was measured at different pH levels by varying the addition of (a) NH_4OH and (b) NaOH solution. XRD patterns of the recovered nanopowder produced from the precipitating agents (c) NH_4OH and (d) NaOH.

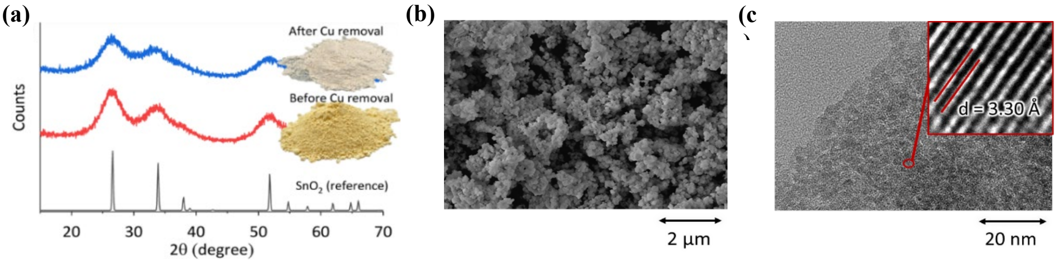

Figure 5. Characterisation of the SnO_2 NPs before and after 1 mol L^{-1} HNO_3 treatment. (a) XRD patterns and images of the SnO_2 nanoparticles before and after copper removal. (b), and (c) present the morphological characteristics of the final SnO_2 NP product (post-copper removal) by SEM and TEM, respectively.

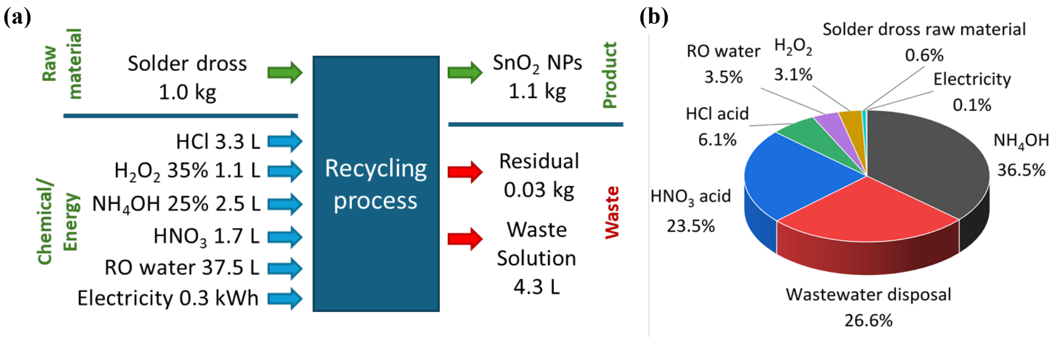

Figure 6. Charts of (a) overall input and output, and (b) cost percentage of the process (calculated from prices of chemicals and energy; see Table S1 for more details).

Table 1. Chemical composition of SnO_2 NPs before and after the copper removal (WD-XRF analysis).

Element	**Element content (wt.%)**	
	Precipitated SnO_2 NPs with NH_4OH	**SnO_2 NPs after Cu removal**
Sn	67.86 (±1.31)	78.42 (±0.05)
O	22.28 (±2.75)	21.14(±0.01)
Cl	8.51 (±1.07)	0.13 (±0.10)
Cu	0.96 (±0.25)	0.085 (±0.02)
Zn	-	-
Fe	0.14 (±0.08)	0.025 (±0.01)
Al	0.035 (±0.01)	0.08 (±0.03)
Si	0.125 (±0.05)	0.1 (±0.01)
Other	0.11 (±0.06)	0.03 (±0.01)

determined from the wt% of Sn and O from the WD-XRF result. The results indicated a remarkable purity of ca. 99.5% for the final SnO_2 NP product. Overall, the tin recovery yield from the initial solder dross was approximately 99.7%, calculated by comparing the wt% of tin in the final product and initial raw material.

Figure 6(a) provides a comprehensive overview of the recycling process, detailing the input and output materials. The process started with 1 kg of tin solder dross and yielded 1.1 kg of SnO_2 nanoparticles. A detailed breakdown of the chemical reagents employed in each step can be found in Figure S5. A cost analysis presented in Figure 6(b), highlights the significant financial implications of the recycling process. The primary expense was the chemicals used (ca. 72.7% of the total cost), followed by the disposal of secondary waste solutions (ca. 26.6%). It is important to note that equipment and worker costs were not included in this analysis. As anticipated, the hydrometallurgical process was dominated by the costs associated with chemicals and waste disposal. The material balance and preliminary cost analysis presented here can serve as a valuable foundation for estimating revenue and profit for scaling up the process to industrial levels. The hydrometallurgical synthesis of SnO_2 NPs presents a potentially advantageous alternative to conventional carbothermic reduction that requires high-temperature smelting (900°C to 1400°C), reduces stannic oxide to crude metal tin, generating slag and necessitating subsequent electrolytic refining for purification [31-33]. In contrast, hydrometallurgical routes offer near-ambient temperature operation and selective metal leaching. However, a critical consideration is the generation of aqueous waste streams, necessitating either rigorous disposal protocols or implementing effective metal recovery strategies to minimise environmental impact and maximise resource utilisation. Additionally, The waste solution obtained after the purification process in this study exhibits substantial copper concentrations, presenting an opportunity for resource recovery. Specifically, the copper-rich solution may be subjected to further processing to yield value-added products. For instance, synthesising copper sulfate crystals, a compound with diverse applications spanning agriculture, electronics, water infrastructure, and healthcare, is a viable route [33]. Alternatively, electrochemical extraction via electrowinning offers a pathway to produce high-purity metallic copper [34,35].

4. Conclusions

This study presents a low-temperature hydrometallurgical process for producing SnO_2 NPs from waste solder dross obtained from a dipping bath process. The method involves a three-step approach: leaching with HCl aqueous solution and H_2O_2 followed by precipitation with NH_4OH and subsequent purification with HNO_3 aqueous solution for Cu removal. The optimised leaching conditions were determined to be 4 $mol \cdot L^{-1}$ HCl, 11% v/v H_2O_2 at 25°C for 15 min. Precipitation of SnO_2 NPs was achieved at pH 4 using NH_4OH, followed by Cu removal by leaching with a 1 $mol \cdot L^{-1}$ HNO_3 aqueous solution for 6 h. This resulted in approximately 99.7% recovery of tin as SnO_2 NPs with a purity of 99.5%. A preliminary cost analysis revealed that the primary expenses were associated with chemicals and waste disposal, accounting for 72.7% and 26.6% of the total cost, respectively. The proposed hydrometallurgical process offers an economically viable solution for recovering valuable metals from waste solder dross, contributing to a circular economy and generating a new product from an electronic process.

Acknowledgements:

The authors would like to thank the Department of Primary Industries and Mines, Thailand for funding and collaboration. Furthermore, the authors acknowledge support from the Innovative Processing and Recycling of Metals Research Center (IPRMRC), Suranaree University of Technology, Thailand.

References

[1] N. Kumar, and A. Maurya, "Development of lead free solder for electronic components based on thermal analysis," *Materials Today: Proceedings,* vol. 62, pp. 2163-2167, 2022..

[2] P. D. Sonawane, V. K. Bupesh Raja, K. Palanikumar, E. A. Kumar, N. Aditya, and V. Rohit, "Effects of gallium, phosphorus and nickel addition in lead-free solders: A review," *Materials Today: Proceedings,* vol. 46, pp. 3578-3581, 2021.

[3] S. Jayesh, and J. Elias, "Experimental investigation on the effect of Ag addition on ternary lead free solder alloy –Sn–0.5Cu–3Bi," *Metals and Materials International,* vol. 26, no. 1, pp. 107-114, 2020.

[4] S. Cheng, C.-M. Huang, and M. Pecht, "A review of lead-free solders for electronics applications," *Microelectronics Reliability,* vol. 75, pp. 77-95, 2017.

[5] A. K. Gain, and L. Zhang, "Growth mechanism of intermetallic compound and mechanical properties of nickel (Ni) nanoparticle doped low melting temperature tin–bismuth (Sn–Bi) solder," *Journal of Materials Science: Materials in Electronics,* vol. 27, no. 1, pp. 781-794, 2016.

[6] M. Sarkar, F. Gulshan, A. R. M. H. Rashid, and M. Hasanuzzaman, "A review of TiO_2-nanoparticle reinforced lead-free solder composites used in electronic components soldering," in *Encyclopedia of Materials: Electronics*, A. S. M. A. Haseeb Ed. Oxford: Academic Press, 2023, pp. 456-463

[7] H. M. Henao, C. Masuda, and K. Nogita, "Metallic tin recovery from wave solder dross," *International Journal of Mineral Processing,* vol. 137, pp. 98-105, 2015.

[8] I. García-Díaz, F. J. Alguacil, and F. A. López, "Tin and silver recovery from wave soldering dross," *Waste Management & Research,* vol. 36, no. 12, pp. 1201-1209, 2018.

[9] Z. Harangi, "Extraction of tin from oxidised soldering dross by carbothermic reduction and acid leaching," *Materials Science and Engineering,* vol. 39, 2014.

[10] S.-h. Lee, K. Yoo, M. K. Jha, and J.-c. Lee, "Separation of Sn from waste Pb-free Sn–Ag–Cu solder in hydrochloric acid solution with ferric chloride," *Hydrometallurgy,* vol. 157, pp. 184-187, 2015.

[11] K. Yoo, J-C. Lee, K-S Lee, B-S. Kim, M-S. Kim, and B. D. Pandey, "Recovery of Sn, Ag and Cu from waste Pb-free solder using nitric acid leaching," *Materials Transactions,* vol. 53, no. 12, pp. 2175-2180, 2012.

[12] S. Kim, J.-c. Lee, K.-s. Lee, K. Yoo, and R. D. Alorro, "Separation of tin, silver and copper from waste pb-free solder using hydro-chloric acid leaching with hydrogen peroxide," *Materials Transactions,* vol. 55, no. 12, pp. 1885-1889, 2014.

[13] M. A. Dheyab, A. A. Aziz, M. S. Jameel, and N. Oladzadabbasabadi, "Recent advances in synthesis, modification, and potential application of tin oxide nanoparticles," *Surfaces and Interfaces,* vol. 28, p. 101677, 2022.

[14] S. Arya, M. Riyas, A. Sharma, B. Singh, Prerna, P. Bandhoria, S. Khan, and V Bharti, "Electrochemical detection of ammonia solution using tin oxide nanoparticles synthesised via sol–gel route," *Applied Physics A,* vol. 124, no. 8, p. 538, 2018.

[15] S. R. Mishra, and M. Ahmaruzzaman, "Tin oxide based nano-structured materials: synthesis and potential applications," *Nanoscale,* vol. 14, no. 5, pp. 1566-1605, 2022.

[16] P. Liu, and V. Sivakov, "Tin/Tin oxide nanostructures: Formation, application, and atomic and electronic structure peculiarities," *Nanomaterials,* vol. 13, no. 17, p. 2391, 2023.

[17] J. Kharbanda, and R. Priya, "Synthesis and applications of tin oxide nanoparticles: An overview," *Materials Today: Proceedings,* vol. 68, pp. 916-921, 2022.

[18] J. Mayandi, M. Marikkannan, V. Ragavendran, and P. Jayabal, "Hydrothermally synthesised Sb and Zn doped SnO_2 nano-particles," *Journal of Nanoscience and Nanotechnology,* vol. 2, pp. 707-710, 2014.

[19] O. A. Fouad, G. Glaspell, and M. S. EL-Shall, "Structural, optical and gas sensing properties of ZnO, SnO_2 and ZTO nanostructures," *Nano,* vol. 05, no. 04, pp. 185-194, 2010.

[20] M. Kandasamy, A. Seetharaman, D. Sivasubramanian, A. Nithya, K. Jothivnkatachalam, N. Maheswari, M. Gopalan, S. Dillibabu, and A. Eftekhari, "Ni-doped SnO_2 nanoparticles for sensing and photocatalysis," *ACS Applied Nano Materials,* vol. 1, no. 10, pp. 5823-5836, 2018.

[21] T. Entradas, J. F. Cabrita, S. Dalui, M. R. Nunes, O. C. Monteiro, and A. J. Silvestre, "Synthesis of sub-5 nm Co-doped SnO_2 nanoparticles and their structural, microstructural, optical and photocatalytic properties," *Materials Chemistry and Physics,* vol. 147, no. 3, pp. 563-571, 2014.

[22] M. Madhumala, D. Madhavi, T. Sankarshana, and S. Sridhar, "Recovery of hydrochloric acid and glycerol from aqueous solutions in chloralkali and chemical process industries by membrane distillation technique," *Journal of the Taiwan Institute of Chemical Engineers,* vol. 45, no. 4, pp. 1249-1259, 2014.

[23] C. McKinley, and A. Ghahreman, "Hydrochloric acid regeneration in hydrometallurgical processes: a review," *Mineral Processing and Extractive Metallurgy,* vol. 127, no. 3, pp. 157-168, 2018.

[24] S.-k. Kim, J.-c. Lee, and K. Yoo, "Leaching of tin from waste Pb-free solder in hydrochloric acid solution with stannic chloride," *Hydrometallurgy,* vol. 165, pp. 143-147, 2016.

[25] S. Li, J. Ma, F. Xu, L. Wei, and D. He, "Fundamental principles and environmental applications of electrochemical hydrogen peroxide production: A review," *Chemical Engineering Journal,* vol. 452, p. 139371, 2023.

[26] S. Ghosh and S. Roy, "Effect of ageing on $Sn_6O_4(OH)_4$ in aqueous medium—simultaneous production of SnO and SnO_2 nanoparticles at room temperature," *Journal of Sol-Gel Science and Technology,* vol. 81, no. 3, pp. 769-773, 2017.

[27] J. Geurts, S. Rau, W. Richter, and F. J. Schmitte, "SnO films and their oxidation to SnO2: Raman scattering, IR reflectivity

and X-ray diffraction studies," *Thin Solid Films,* vol. 121, no. 3, pp. 217-225, 1984.

[28] Z. T. Ichlas, R. A. Rustandi, and M. Z. Mubarok, "Selective nitric acid leaching for recycling of lead-bearing solder dross," *Journal of Cleaner Production,* vol. 264, p. 121675, 2020.

[29] V. P. Sankara Narayanan, S. G. Kathirason, P. Elango, R. Subramanian, S. R, and A. Gurusamy, "Emilia sonchifolia leaf extract-mediated green synthesis, characterisation, in vitro biological activities, photocatalytic degradation and in vivo Danio rerio embryo toxicity of copper nanoparticles," *RSC Advances,* vol. 13, no. 24, pp. 16724-16740, 2023.

[30] M. Karmaoui, A. B. J. Sobrido, P. McMillan, A. E. Aliev, R. C. Pullar, J. A. Labrincha, and D. M. Tobaldi, "One-step synthesis, structure, and band gap properties of SnO_2 nanoparticles made by a low temperature nonaqueous sol-gel technique," (in eng), *ACS Omega,* vol. 3, no. 10, pp. 13227-13238, 2018.

[31] A. Y. Fosu, D. Bartier, F. Diot, and N. Kanari, "Insight into the extractive metallurgy of tin from cassiterite," *Materials,* vol. 17, no. 13, p. 3312, 2024,.

[32] Z. Su, Y. Zhang, B. Liu, M. Lu, G. Li, and T. Jiang, "Extraction and separation of tin from tin-bearing secondary resources: A review," *JOM,* vol. 69, no. 11, pp. 2364-2372, 2017.

[33] S. Khumkoa, N. Ma-ud, T. Patcharawit, and T. Yingnakorn, "Tin, silver, and copper sulfate compound extraction from lead-free solder dross by reduction with petroleum coke, electrorefining, cementation, and crystallisation process," *Journal of Metals, Materials and Minerals,* vol. 34, no. 4, p. 2007, 2024.

[34] N. Ma-ud, S. Khumkoa, P. Buahombura, W. Piyawit, T. Patcharawit, S. Thongnak, and T. Yingnakorn, "Study on recycling of galvanic sludge containing copper for pure copper production," *Journal of Material Sciences & Engineering,* vol. 8, no. 2169-0022, 2019.

[35] T. Patcharawit, C. Kansomket, N. Wongnaree, W. Kritsrikan, T. Yingnakorn, and S. Khumkoa, "Hybrid recovery of copper and silver from PV ribbon and Ag finger of EOL solar panels," *Energy and Power Engineering,* vol. 16, no. 6, pp. 89-99, 2022.